



Published in final edited form as:

Arch Oral Biol. 2008 August ; 53(8): 785–790.

Comparative Properties of Recombinant Human and Bovine Matrix Metalloproteinase-20

Li Zhu^a, Katoro Tanimoto^a, Sarah Robinsin^b, James Chen^a, Ewa Witkowska^{b,c}, Steve Hall^{b,c}, Thuan Le^a, Pamela K. DenBesten^a, and Wu Li^{a*}

^aDepartment of Orofacial Sciences, University of California, San Francisco, 513 Parnassus Avenue, San Francisco, CA 94143

^bDepartment of Cell and Tissue Biology, University of California, San Francisco, 513 Parnassus Avenue, San Francisco, CA 94143

^cBiomolecular Resource Center Mass Spectrometry Facility, University of California, San Francisco, 513 Parnassus Avenue, San Francisco, CA 94143

Abstract

Introduction—Matrix Metalloproteinase-20 (MMP-20) is a predominant enzyme for the progressive processing of enamel extracellular matrix protein components (primarily amelogenin) during the early stages of enamel formation. So far, the recombinant porcine, mouse and bovine MMP-20 have been cloned and used extensively in the researches of tooth enamel development. The homology of these MMP-20s to human MMP-20 is approximately 80%. The effect of sequence differences on the properties of these enzymes is poorly understood even though they have been used to hydrolyze amelogenins from different species.

Objective—Our goal is to compare the characteristics between recombinant human MMP-20 (rhMMP-20) and bovine MMP-20 (rbMMP-20).

Design—rhMMP-20 and rbMMP-20 were parallelly expressed, purified and activated. The SDS-PAGE, zymography and quenched peptide assay were used for characterization and comparisons.

Results—Both proteases were activated by autocatalysis in a similar pattern of fragmentation. Dynamically, rbMMP-20 autoactivated faster and digested a fluorescence-quenched peptide Mca-PLGL-Dpa-AR, a non-amelogenin substrate, more efficiently than rhMMP-20. However, rhMMP-20 showed higher enzymatic activity for a human amelogenin substrate and in addition, it created an extra cleavage site at its C-terminus.

Conclusions—The differences in their catalytic properties and substrate specificities may be attributed to the sequence divergence of MMP-20 between species, especially in the hinge region.

Keywords

MMP-20; cross-species comparison; substrate specificity; catalytic properties

Corresponding author: Wu Li, Department of Orofacial Sciences, University of California, San Francisco, 513 Parnassus Avenue, Box #0422, San Francisco, CA 94143, U.S.A, Tel: 415-502-7829, Fax: 415-476-4204, Email: wu.li@ucsf.edu.

Publisher's Disclaimer: This is a PDF file of an unedited manuscript that has been accepted for publication. As a service to our customers we are providing this early version of the manuscript. The manuscript will undergo copyediting, typesetting, and review of the resulting proof before it is published in its final citable form. Please note that during the production process errors may be discovered which could affect the content, and all legal disclaimers that apply to the journal pertain.

1. Introduction

Matrix metalloproteinase-20 (MMP-20) belongs to a superfamily of zinc-dependent metallo-peptidases involved in tissue remodeling (1). MMP-20 has the characteristic domain structure of most other MMPs, including a signal peptide, a prodomain that maintains enzyme latency, a catalytic domain with a zinc and calcium binding sites, and C-terminal hemopexin domains. MMP-20 appears to be the only MMP that exhibits an entirely tooth-specific expression pattern (2).

Within developing teeth, MMP-20 is secreted by ameloblasts during the early to mid stages of amelogenesis, and participates in the stepwise processing of enamel matrix proteins to facilitate the crystal growth (3). Amelogenin is the most abundant enamel matrix protein. Proteolysis experiments have shown that MMP-20 cleaves amelogenin to generate predominantly the tyrosine-rich amelogenin polypeptide (TRAP) and 20 kDa amelogenin peptide (Amg20) (4, 5). Amelogenesis imperfecta phenotype observed in MMP-20 deficient mice further supports the essential role of MMP-20 during initial stages of enamel formation (6).

To date, MMP-20 has been successfully cloned from porcine and bovine enamel organs (7) (8), mature human odontoblasts (3), and mouse incisor (9). Studies have shown that recombinant MMP-20s are capable of degrading amelogenin *in vitro* under physiological conditions (3,5,7,10). Recombinant MMP-20 produces a pattern of amelogenin cleavages virtually identical to those observed *in vivo* (5). However, Ryu *et al.* showed that rodent amelogenin was cleaved into more and smaller fragments by recombinant porcine MMP-20 than its pig homologue (5), reflecting species differences in substrate susceptibility.

Recombinant porcine, mouse and bovine MMP-20s have been used extensively in the studies of enamel formation so far (5,7,11,12). In our previous publications (13), we used recombinant bovine MMP-20 to cleave human recombinant amelogenin. Though MMP-20s from various species are approximately 80% homologous to human MMP-20 (9), the effect of sequence divergence on the enzyme properties is still largely unknown. To gain a deep insight into MMP-20 activity across species, the present study aims to compare the proteolytic properties and substrate specificity between recombinant human MMP-20 (rhMMP-20) and bovine MMP-20 (rbMMP-20).

2. Materials and Methods

2.1. Synthesis and purification of recombinant human and bovine MMP-20

Bovine MMP-20 cDNA was cloned into pRSET A vector as described before (11). cDNA encoding human MMP-20 was amplified by PCR from RNA isolated from human fetal tooth tissues through a tissue shared program in University of California at San Francisco, CA, USA. PCR was performed with primers 5'-ATGAAGGTGCTCCCTGCATC-3' and 5'-TAGCAACCAATCCAGGA ACTA-3' in a 5-min initial denaturation at 95°C, followed by 30 cycles of amplification (denaturing at 94°C for 30 s, annealing at 55°C for 30 s, extension at 72°C for 1 min and last extension cycle at 72°C for 7 min). The original PCR fragment was cloned into pCR 2.1 TOPO vector (Invitrogen, Carlsbad, CA, USA). After sequence confirmation, the cloned fragment was excised from pCR2.1 vector by PCR using primers 5'-TGGGCAGCCTC CCCCAGGAC-3' and 5'-GCTTTT CCGGTA CCTTAGCAACC-3'. PCR was carried out with Taq polymerase. The amplified product was digested with Kpn I and subsequently subcloned into the expression vector pRSET B (Invitrogen). The resulting bovine and human pRSET-MMP20 was then transformed into competent *E. coli* BL21(DE3), and was induced with 0.8 mM isopropyl-1-thio- β -galactopyranoside (IPTG) at 25°C for 16 h. The expressed recombinant proteins were purified by using nickel resin (ProBond, Invitrogen) under denaturing conditions in accordance with the manufacturer's instructions. The purified

rhMMP-20 proenzyme was activated by stepwise dialysis against decreasing amounts of urea in 20mM Tris buffer pH 7.5 containing 50 μM ZnCl_2 , 5mM CaCl_2 , 150mM NaCl at 4°C, as described in our previous publication (11).

2.2. SDS-PAGE zymography

To determine protease activity, zymography were done using 12% SDS-PAGE gels co-polymerized with 1 mg/ml purified recombinant human amelogenin (rh174) (11). rhMMP-20 and rbMMP-20 were treated with sample buffer without heating and then separated by SDS-PAGE. After electrophoresis, the gels were soaked in 2.5% Triton X-100 for 1 hour at room temperature to remove the sodium dodecyl sulfate, and incubated in reaction buffer (50mM Tris-HCl, 150mM NaCl, 10mM CaCl_2 , 10 μM ZnCl_2 , pH 7.5) at 37°C overnight to allow proteinase to digest its substrate. Gels were stained with 0.5% Coomassie brilliant blue R-250 in 40% methanol and 10% acetic acid for 1 hour, and destained with 40% methanol and 10% acetic acid. Proteolytic activities appeared as clear bands of hydrolysis against a dark background of stained amelogenin. The densitometry of substrate lysis zones was measured by using a NIH Image software (version 1.63; National Institutes of Health, Bethesda, Md.).

2.3. Quenched peptide assay

The fluorescence-quenched peptide Mca-PLGL-Dpa-AR (Bachem California, CA, USA,) at a concentration of 5 μM was incubated at 37°C with or without activated rhMMP-20 and rbMMP-20 in reaction buffer. Assays were configured in black opaque plates in final reaction volumes of 200 μl . The fluorescence intensity of the enzymatic products was measured by a Spectra Max GEMINI XS fluorometer (Molecular Devices, Sunnyvale, CA, USA) using the excitation wavelength at 325 nm and the emission wavelength at 395 nm. The Michaelis-Menten constant K_m and the maximum velocity V_{max} were calculated from Lineweaver-Burk ($1/S$ versus $1/V$) plots. K_{cat} values were calculated from the V_{max} values which represent the maximal turnover rate. All reported kinetic values are averages of at least three independent assays.

2.4. Western blotting

Activated recombinant human and bovine MMP-20, 4 μg per lane, were separated by 12% SDS-PAGE and blotted onto nitrocellulose membrane (GE Healthcare, Piscataway, NJ, USA). After 1 h blocking, the membranes were probed with rabbit anti-human MMP-20 antibody (Sigma, ST. Louis, MO, USA) and species-specific horseradish peroxidase-conjugated secondary antibody (Sigma), followed by exposure to enhanced chemiluminescence detection reagents (GE Healthcare) for 1 minute. Blots were then processed for autoradiography.

2.5. Mass spectrometry analysis

The proteases (rhMMP-20 and rbMMP-20) were incubated with rh174 at a molar ratio of 1:1000 in the reaction buffer at 37°C. After 1 h incubation, the reactions were stopped by adding equal amount of 0.1% TFA. Mass spectrometric analyses were carried out on a Voyager DE STR MALDI-TOF MS (Applied biosystems, Foster City, CA) with N_2 laser in either linear (m/z 1000 – 25,000) or reflector (m/z 800 – 6000) positive ion mode. Samples were mixed 1:1 directly on the MALDI stainless steel target with 5 mg mL^{-1} α -Cyano-4-hydroxycinnamic acid in 50% MeCN/0.1% TFA matrix. External optimized calibration (OptiPlate, Applied Biosystems) was based on four peptide standards within m/z 1290–3800 (angiotensin I and three ACTH clips: 1–17, 18–30 and 7–38) for reflector data and m/z 5700–17000 (insulin, thioredoxin and apomyoglobin) for linear data. Spectra were processed with Data Explorer 4.0 software (Applied Biosystems) by performing baseline adjustment, noise filtering and de-isotoping.

3. Results

3.1. Expression, purification and activation of recombinant MMP-20s

To compare their catalytic characteristics and activation mechanisms, parallel expression and purification of rhMMP-20 and rbMMP-20 were accomplished. Following induction with IPTG, both MMP-20s were found highly expressed in *E. coli* as insoluble inclusions (Fig. 1). After solubilization in 6 M guanidine-HCl, both human and bovine proMMP-20s could be purified under denaturing conditions to give a major band at molecular mass of 55 kDa when analyzed by SDS-PAGE (Fig. 2).

Refolding of the denatured pro-enzyme was achieved through sequential removal of urea by dialysis against buffer with zinc. It was observed that the proMMP-20 of both species underwent autolytic activation during the refolding process. After the final dialysis step, human pro-MMP-20 autolytically proceeded into a major fragment at 25 kDa and along with other minor bands of 43, 21 and 18 kDa (lane 2 in Fig 3). Though autoproteolytic cleavage of bovine proMMP-20 also generated the 43, 25, and 18 kDa bands, its major fragment is 21 kDa (lane 3 in Fig. 3). All the fragments could be detected by western blot with anti-human MMP-20 antibody (Fig. 4).

3.2. Enzymatic activity of MMP-20s

The purity of the human and bovine MMP-20 was compared on SDS-PAGE, and there was no significant difference in purity between the two proteins (Fig. 3 A). Therefore, the difference in enzymatic activity of the two proteins should represent their species specificities.

The data of the quenched peptide hydrolysis by rbMMP-20 and rhMMP-20, measured at substrate concentrations of 2.5, 3.75, and 5 μM at 37°C, were used to calculate the enzymatic kinetics of these two enzymes. As shown in table 1, rhMMP-20 has a K_m of 16.3 μM , revealing a significantly lower affinity for the peptide substrate than demonstrated by its bovine analogue. In addition, rhMMP-20 has a slightly slower K_{cat} ($8.1 \times 10^3 \text{ S}^{-1}$), resulting in a K_{cat}/K_m of $4.9 \times 10^5 \text{ M}^{-1} \cdot \text{S}^{-1}$ that was 1.3 fold less than the value for rbMMP-20 ($6.3 \times 10^5 \text{ M}^{-1} \cdot \text{S}^{-1}$).

Zymography disclosed that the 43, 25, 21 and 18 kDa autolyzed products of both human and bovine MMP-20 could catalyze the degradation of rh174 substrates (Fig. 4). With the NIH image program, the activities of MMP-20 were determined by quantitation of hydrolytic zones on amelogenin substrate gels. The fragments of 21 and 25 kDa in both MMP-20s demonstrated the strongest activity among the autolytic products (Fig. 4). Densitometric measurements indicated that the total hydrolytic zones of 21 plus 25 kDa rhMMP-20 were approximately 2 fold and 1.5 fold higher, respectively, as compared to rbMMP-20.

3.3. Comparisons of rhMMP-20 and rbMMP-20 cleavage sites in human amelogenin

To compare the digestion pattern, the rh174 was incubated at 37°C with rhMMP-20 and rbMMP-20, respectively. The MMP-20 cleavage sites on rh174 sequence were determined by MALDI-TOF mass spectrometry. Mass spectra of the digestion products identified that the rbMMP-20 and rhMMP-20 processed rh174 at nearly identical sites, except that the later one introduced an extra cleavage site between T¹⁵⁹ and L¹⁶⁰ (Table 2). The most identified cleavage sites by rhMMP-20 and rbMMP-20 were located at N- and C-terminal regions of rh174.

4. Discussion

Bovine MMP-20 consists of 481 amino acids, and is slightly less homologous to human MMP-20 than to its mouse and porcine counterparts (9). The catalytic domain of MMP-20 was highly conserved (> 90% identity) between human and bovine, but the hinge region varied

substantially with 70% homology, which may lead to diversity of protein characteristics between species (9).

Both rhMMP-20 and rbMMP-20 were expressed in *E coli* with high efficiency, and purified by nickel affinity chromatography under denature condition. During refolding in stepwise dialysis, they were activated by autolytic processing in a similar pattern. As shown by SDS-PAGE and western blot, autolytic activation of the proforms of rhMMP-20 and rbMMP-20 yielded the fragments at similar size. These fragments correlated with the expected sizes of entire catalytic domain plus different domains at its C-terminus. These data are consistent with previous characterization of rbMMP-20 (12). The 43 kDa fragment extends from the start of catalytic domain to the C-terminus of MMP-20. The size of the 21 kDa fragment corresponded to the catalytic domain and hinge region. The 25 kDa cleavage product had an extra hemopexin domain 1, when compared to the 21 kDa fragment. However, the autolysis rates of rhMMP-20 were slower than rbMMP-20, as more 25 kDa products of rbMMP-20 remained after activation under the same conditions. Their difference in the rate of autoactivation may reflect species specificity.

It is known that MMP-20 becomes functionally active when proteolytic cleavage removes the pro-domain to expose the zinc atom and free the active site for the enzyme to interact with its substrate. The autolysis fragments of rhMMP-20 and rbMMP-20 displayed various enzymatic activities on amelogenin-zymography. For both enzymes, the fragments with highest activity were 25 and 21 kDa that contain the catalytic domain and hinge region (12), while less activity was observed for the autolytic fragment at 18 kDa. This observation suggested that catalytic domain and hinge region together are essential to maintain the highest catalytic activity of MMP-20.

Our work also indicated that both rhMMP-20 and rbMMP-20 could efficiently digest the universal fluorescence quenched peptide and rh174, but they showed different preference to these substrates. rbMMP-20 cleaved the quenched peptide with higher velocity and stronger affinity than its human analogue. However, densitometry analysis of hydrolytic bands on the substrate zymography gels showed that rbMMP-20 hydrolyzed less rh174 amelogenin substrates than rhMMP-20. The differential substrate preference suggests that a few amino acid changes in the primary sequences of MMP-20, particularly in the hinge region, might contribute to the species differences found in enzyme and substrate interactions.

Mass spectrometry analysis showed that rh174 was targeted by rhMMP-20 and rbMMP-20 primarily at its N- and C-terminal regions (Table 2), generating TRAP, Amg20 and other proteolytic fragments. In comparison with bovine analogue, rhMMP-20 introduced an extra proteolysis site between T¹⁵⁹ and L¹⁶⁰, indicating that it has relatively stronger proteolytic activity against amelogenin substrate from the same species and hence creates more cleavages. This discrepancy also suggests that cognate MMP-20 from different species may differ in substrate recognition and cleavage.

In summary, while recombinant human and bovine MMP-20 share many similarities, some differences do exist between them, such as autoactivation speed and substrate preference. These differences may arise from the sequence divergence of MMP-20 between species, especially in the hinge region. Likewise, a comparative study demonstrates that the catalytic properties and substrate specificity of rat MMP-12 differed from those of human MMP-12 (14). Taken together, these findings enhance our understanding of enzymatic properties of MMP-20 across species. Such information would be useful for selecting the appropriate MMP-20 member in the studies of enamel formation.

Acknowledgments

This work was supported by R01 DE015821 grant from the National Institute of Dental and Craniofacial Research, and by the SANDLER New Technologies Fund.

References

1. Birkedal-Hansen H, Moore WG, Bodden MK, Windsor LJ, Birkedal-Hansen B, DeCarlo A, et al. Matrix metalloproteinases: a review. *Crit Rev Oral Biol Med* 1993;4(2):197–250. [PubMed: 8435466]
2. Palosaari H, Pennington CJ, Larmas M, Edwards DR, Tjaderhane L, Salo T. Expression profile of matrix metalloproteinases (MMPs) and tissue inhibitors of MMPs in mature human odontoblasts and pulp tissue. *Eur J Oral Sci* 2003;111(2):117–127. [PubMed: 12648263]
3. Llano E, Pendas AM, Knauper V, Sorsa T, Salo T, Salido E, et al. Identification and structural and functional characterization of human enamelysin (MMP-20). *Biochemistry* 1997;36(49):15101–15108. [PubMed: 9398237]
4. Fincham AG, Moradian-Oldak J. Amelogenin post-translational modifications: carboxy-terminal processing and the phosphorylation of bovine and porcine "TRAP" and "LRAP" amelogenins. *Biochem Biophys Res Commun* 1993;197(1):248–255. [PubMed: 8250931]
5. Ryu OH, Fincham AG, Hu CC, Zhang C, Qian Q, Bartlett JD, et al. Characterization of recombinant pig enamelysin activity and cleavage of recombinant pig and mouse amelogenins. *J Dent Res* 1999;78(3):743–750. [PubMed: 10096449]
6. Caterina JJ, Skobe Z, Shi J, Ding Y, Simmer JP, Birkedal-Hansen H, et al. Enamelysin (matrix metalloproteinase 20)-deficient mice display an amelogenesis imperfecta phenotype. *J Biol Chem* 2002;277(51):49598–49604. [PubMed: 12393861]
7. Bartlett JD, Simmer JP, Xue J, Margolis HC, Moreno EC. Molecular cloning and mRNA tissue distribution of a novel matrix metalloproteinase isolated from porcine enamel organ. *Gene* 1996;183(1–2):123–128. [PubMed: 8996096]
8. Den Besten PK, Punzi JS, Li W. Purification and sequencing of a 21 kDa and 25 kDa bovine enamel metalloproteinase. *Eur J Oral Sci* 1998;106:345–349. [PubMed: 9541246]
9. Caterina J, Shi J, Sun X, Qian Q, Yamada S, Liu Y, et al. Cloning, characterization, and expression analysis of mouse enamelysin. *J Dent Res* 2000;79(9):1697–1703. [PubMed: 11023266]
10. Fukae M, Tanabe T, Uchida T, Lee SK, Ryu OH, Murakami C, et al. Enamelysin (matrix metalloproteinase-20): localization in the developing tooth and effects of pH and calcium on amelogenin hydrolysis. *J Dent Res* 1998;77(8):1580–1588. [PubMed: 9719031]
11. Palosaari H, Ding Y, Larmas M, Sorsa T, Bartlett JD, Salo T, et al. Regulation and interactions of MT1-MMP and MMP-20 in human odontoblasts and pulp tissue in vitro. *J Dent Res* 2002;81(5):354–359. [PubMed: 12097451]
12. Li W, Machule D, Gao C, DenBesten PK. Activation of recombinant bovine matrix metalloproteinase-20 and its hydrolysis of two amelogenin oligopeptides. *Eur J Oral Sci* 1999;107(5):352–359. [PubMed: 10515200]
13. Li W, Gibson CW, Abrams WR, Andrews DW, DenBesten PK. Reduced hydrolysis of amelogenin may result in X-linked amelogenesis imperfecta. *Matrix Biol* 2001;19(8):755–760. [PubMed: 11223334]
14. Fu JY, Lyga A, Shi H, Blue ML, Dixon B, Chen D. Cloning, expression, purification, and characterization of rat MMP-12. *Protein Expr Purif* 2001;21(2):268–274. [PubMed: 11237688]

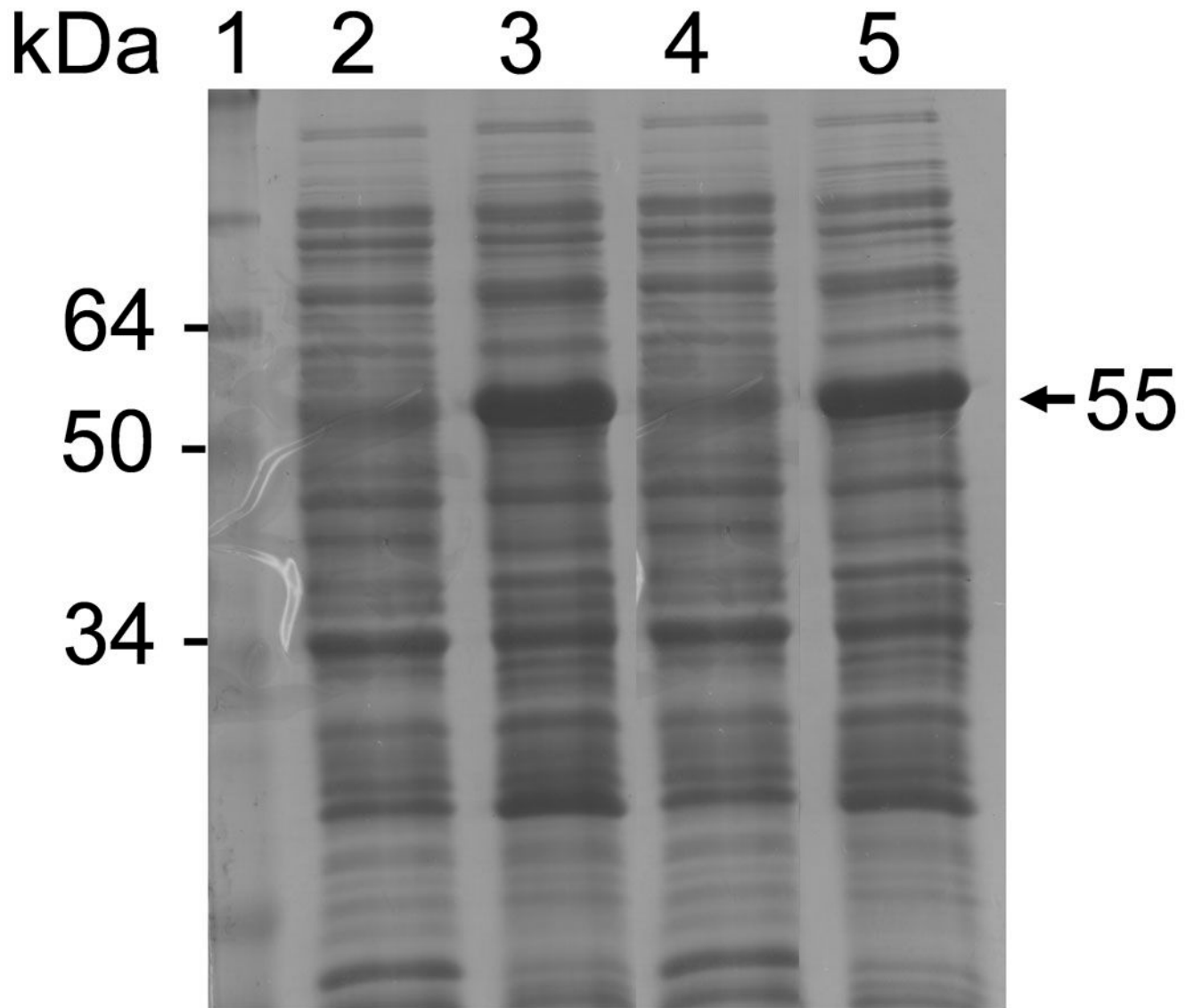


Figure 1. SDS-PAGE analysis of rhMMP-20 and rbMMP-20 expression in *E. coli*. Lane 1, molecular size markers; lane 2 and 4, non-induced controls of rhMMP-20 and rbMMP-20, respectively; lane 3, rhMMP-20 induced by IPTG; lane 5, IPTG induction of rbMMP-20. The arrow indicates induced proteins.

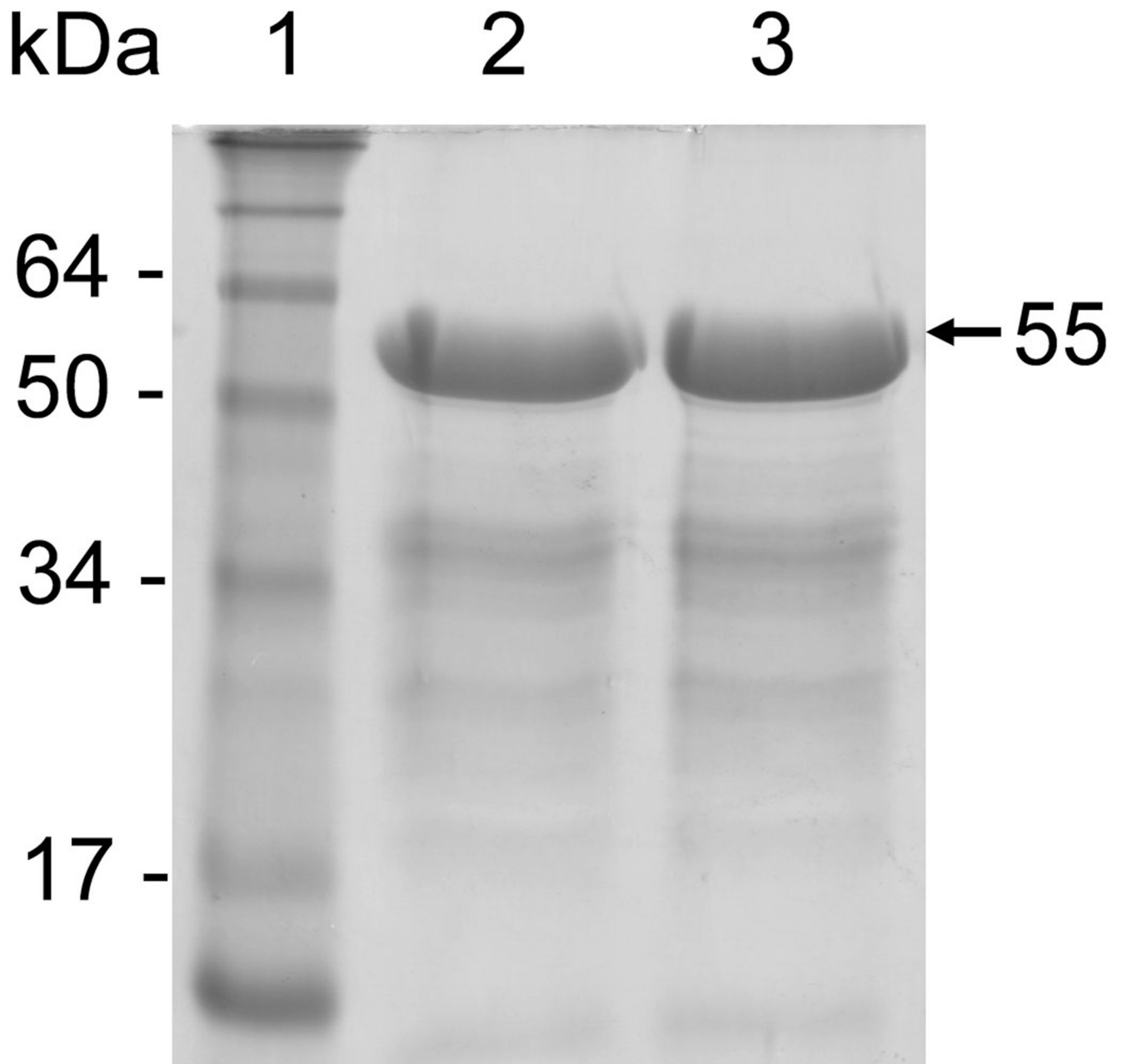


Figure 2. Purified inactive forms of rhMMP-20 and rbMMP-20. Purification of recombinant MMP-20 proteins was performed by nickel affinity chromatography under denaturing conditions. Lane 1, molecular size markers; Lane 2 and 3, affinity purified rhMMP-20 and rbMMP-20, respectively.

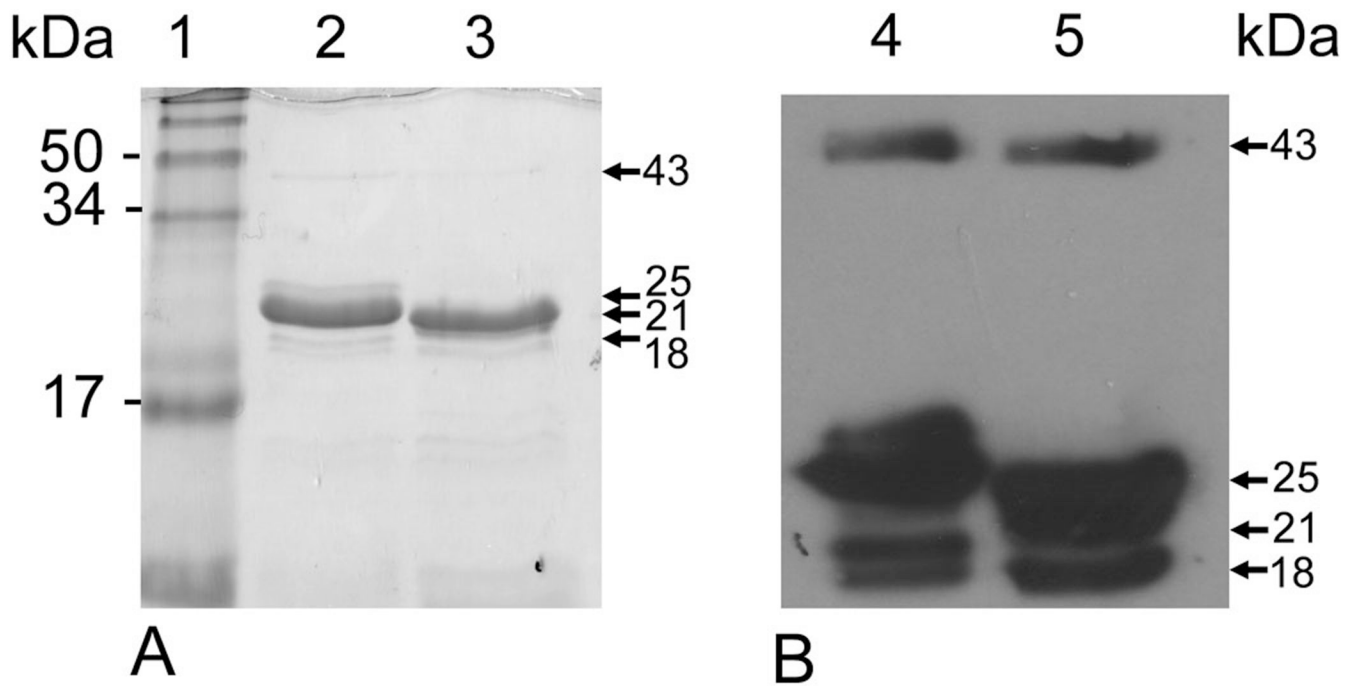


Figure 3. Autolytic activation of rhMMP-20 and rbMMP-20 analyzed by SDS-PAGE (A) and western blot (B). Lane 1, molecular size markers; Lane 2 and 4, active rhMMP-20 after dialysis; lane 3 and 5, active rbMMP-20 after dialysis. The arrows indicate their autolyzed fragments.

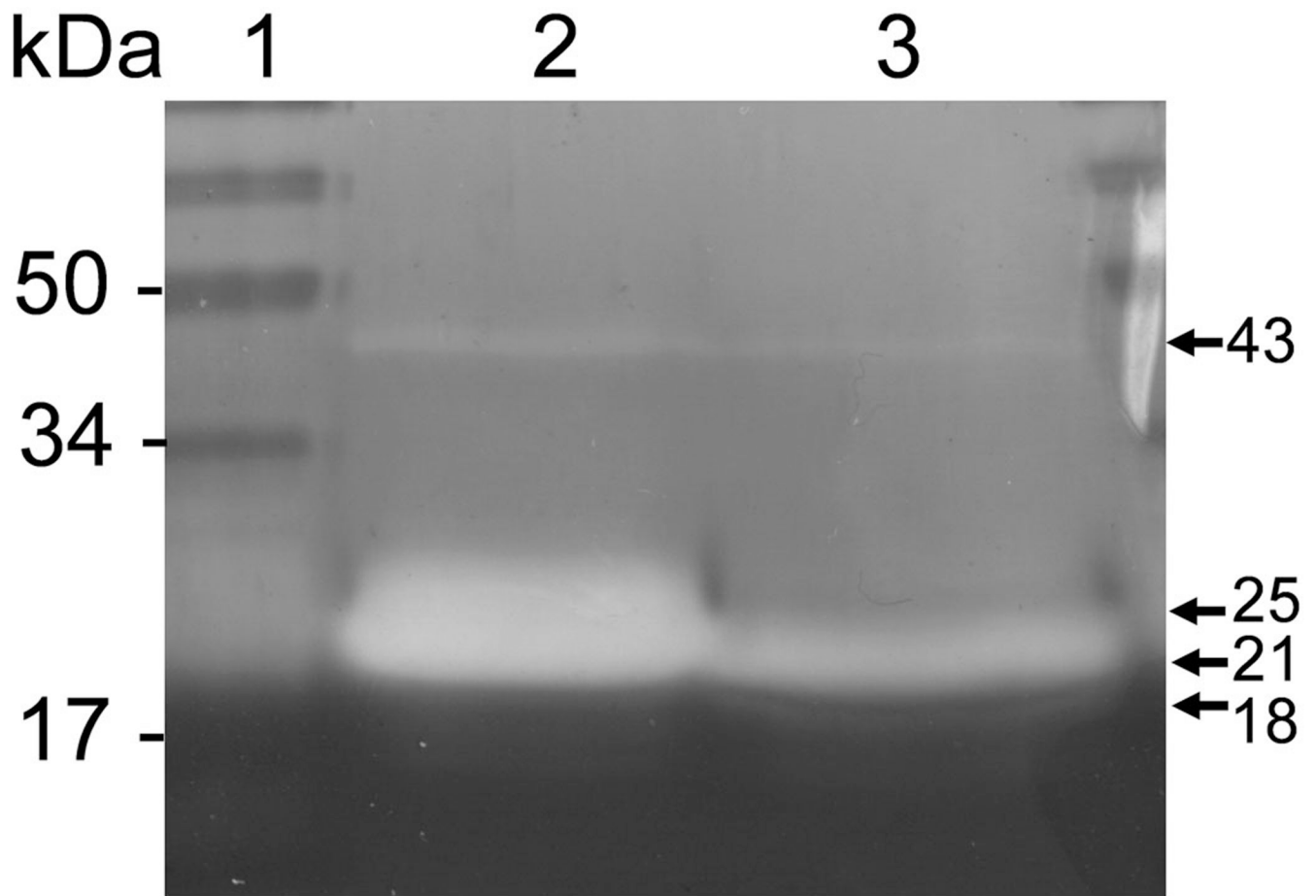


Figure 4. Activity of rhMMP-20 and rbMMP assessed by zymography with rh174 as substrate. Lane 1, molecular size markers; lanes 2 and 3, rhMMP-20 and rbMMP-20 respectively. The arrows indicate the active forms of refolded proteins.

Table 1

Kinetic parameters of rhMMP-20 and rbMMP-20 binding to and/or hydrolysis of quenched peptide Mca-PLGL-Dpa-AR.

Enzyme	K_m (μM)	SD	K_{cat} (s^{-1})	SD	K_{cat}/K_m ($\times 10^5 \text{M}^{-1} \text{s}^{-1}$)
rbMMP-20	14.3	0.36	9.0	0.26	6.3
rhMMP-20	16.4	0.31	8.1	0.20	4.9

Table 2

MALDI-TOF MS predicted and observed m/z ratios of peptides that were generated by digestion of rh174 with both rhMMP-20 and rbMMP-20 respectively. The slash marks indicate the cleavage site.

<i>Cleavage loci</i>	<i>Predicted m/z (monoisotopic)</i>	<i>Range</i>	<i>Observed m/z</i>	
			by rhMMP-20	by rbMMP-20
FSY/EVL	1629.8	2–16	1629.6	1629.6
GGW/LHH	4991.6	2–44	4990.8	4990.5
MFP/MQP	3238.7	147–175	3239.0	3238.9
MLP/DLT	2233.4	156–175	2233.7	2233.8
DLT/LEA	1903.9	159–175	1903.7	----
LTL/EAW	1790.9	160–175	1790.6	1790.5
AWP/STD	1307.6	164–175	1307.4	1307.5